Elastic constants of osmium between 5 and 300 K

C. Pantea,[1] I. Stroe,[1] H. Ledbetter,[2] J. B. Betts,[1] Y. Zhao,[1] L. L. Daemen,[1] H. Cynn,[3] and A. Migliori[1]
[1]*Los Alamos National Laboratory, Los Alamos, New Mexico 87545, USA*
[2]*University of Colorado, Boulder, Colorado 80309, USA*
[3]*Lawrence Livermore National Laboratory, University of California, Livermore, California 94550, USA*
(Received 25 February 2009; revised manuscript received 18 May 2009; published 16 July 2009)

Using two measurement methods, pulse-echo ultrasound and resonance ultrasound spectroscopy, we measured the elastic constants of both monocrystal and polycrystal osmium between 5 and 300 K. Our measurements help to resolve the current measurement-and-theory controversy concerning whether osmium's bulk modulus exceeds diamond's. It does not at any temperature (for osmium, we find a zero-temperature bulk modulus of 410 GPa and a 300 K value of 405 GPa, while diamond's value being 442 GPa). From the zero-temperature elastic constants, we extract a Debye temperature of 477 K. From Grüneisen's first rule, we extract a Grüneisen parameter of 2.1, agreeing well with handbook values. Osmium shows near elastic anisotropy and small elastic constant changes with temperature (for example, the bulk modulus increases only about 1.2% upon cooling through the studied temperature interval). In all cases, the $C_{ij}(T)$ measurements agree well with an Einstein-oscillator model. We consider especially the Poisson ratio, which is low and anisotropic (ν_{12}=0.242, ν_{13}=0.196) and suggests some covalent interatomic bonding, which may account for osmium's extreme high hardness and the departure of the 5*d* elements from Friedel's parabolic bulk-modulus/atomic-number model.

DOI: 10.1103/PhysRevB.80.024112 PACS number(s): 62.20.D−, 63.70.+h, 34.20.Cf

I. INTRODUCTION

Osmium's monocrystal elastic constants provide much interest for many varied reasons: (1) among the 30 *d*-electron transition metals, we lack monocrystal elastic constants for only two: La and Os. This lack is especially surprising because Os shows the highest hardness of any metallic element, much current research proceeds on hardness, and hardness connects strongly with the elastic constants.[1] (2) In recent years, several studies, both measurement and theory, suggested that for osmium the principal elastic constant, the bulk modulus, actually exceeds diamond's, disputing the long-held concept that diamond represents nature's stiffest material. Osmium reported bulk modulus from different high-pressure studies ranging from 390 to 467 GPa, the accepted value for diamond being 442 GPa. To the best of our knowledge, the only available theoretical calculations are by Fast *et al.*,[2] Fan *et al.*,[3] and Minisini *et al.*[4] (3) From accurate zero-temperature elastic constants, one obtains the most reliable Debye temperature,[5] which relates to many mechanical-physical properties.[6,7]

Osmium is a 5*d*-transition element, a group that, along with 4*d*-transition elements, stands out in hardness, being harder than most elements in Mendeleev's table (see, for example, Fig. 1 in Ref. 8). Osmium crystallizes in an hcp crystal structure, which has a denser atomic packing than any other crystal structure, including fcc. (Diamond's crystal structure consists of four interpenetrating fcc lattices.) Diamond's higher hardness results from its covalent interatomic bonding[7] versus osmium's mainly metallic bonding. Hexagonal lattices are characterized by an isotropic close-packed plane and five independent elastic constants, usually taken to be the Voigt coefficients: C_{11}, C_{12}, C_{13}, C_{33}, and C_{44}.

Because resonant ultrasound spectroscopy (RUS) measurements on isotropic polycrystalline samples can only yield two independent elastic constants, we also measured osmium's five independent elastic constants between 300 and 5 K using RUS (Refs. 9–12) on high-quality monocrystalline specimens. RUS is a technique where one acoustic transducer drives the specimen while frequency is swept; peaks in the response of a second transducer determine the mechanical resonances, which are then analyzed to determine the full elastic tensor of the specimen under investigation. The RUS results were confirmed by pulse-echo ultrasound measurements at room temperature and the bulk modulus, absent complications, which is expected to be the same for monocrystal and polycrystal materials was indeed the same within experimental errors.

II. MEASUREMENTS

We obtained oriented monocrystals from Accumet Materials Co., Briarcliff Manor, New York. Polycrystalline shots of 40 mesh were obtained from Alfa Products, Thiokol/Ventron Division, Danvers, Massachusetts. We measured a total of four specimens: two monocrystals and two polycrystals, with sizes of 1–2 mm on one side. All specimens were polished to obtain flat and parallel faces, with sharp 90° edges. We corrected for osmium's thermal expansion following Ref. 13.

Typical pulse-echo measurements determine the two-way travel time of sound in a specimen of known length. The quality of the received signal depends strongly on the flatness and parallelism of the two faces perpendicular to the wave-propagation direction. We used an all-digital ultrasonic pulse-echo-overlap method; details appear in Ref. 14. The transducers used for the pulse-echo experiments were acquired from Boston Piezo-Optics Bellingham, Massachusetts, USA. For compressional mode we used a 40 MHz, 36° Y-cut (*P* wave) $LiNbO_3$ transducer, while for shear mode we

used a 40 MHz, 41° X-cut (*S* wave) $LiNbO_3$ transducer. Both were disk shaped, 3.2 mm diameter, overtone polished, with sputtered Cr/Au electrodes on both sides.

There are several advantages that led us to use RUS as the main method for determining osmium's full elastic tensor: (i) the elastic constants can be determined accurately over a large temperature interval; (ii) the full tensor at given conditions of temperature can be determined from a single measurement on the same crystal; relative errors between moduli introduced by variation in crystal homogeneity, shape, orientation, and size are completely eliminated; (iii) unlike x-ray determination of the bulk modulus at high pressure, there is no need to ensure hydrostatic conditions because the specimens are measured at ambient pressure. Consequently, the extra variable, i.e., pressure, which can introduce additional errors in measurements is eliminated. Most of the previously reported bulk-modulus values are highly scattered between 390 and 467 GPa, depending on how the hydrostaticity was maintained as the pressure was increased during the measurement. Also, the scatter in x-ray measurements (*d* spacings) at different pressures accommodates the use of different B' (first derivative of the bulk modulus with respect to pressure) values in the equation of state, with no (or very small) change in the quality of the fit. These complications present in a high-pressure experiment can introduce errors in the measured values of the elastic constants and are absent with RUS.

The determination of specimen dimensions is a primary factor in the absolute errors of elastic moduli computed from measured quantities in both techniques we used. Corrections for thermal expansion were taken into account based on x-ray diffraction measurements between 77 and 300 K by Finkel' *et al.*[15] We extrapolated their results to 0 K to cover the temperature region of our measurements. The mass density was corrected to 22.61 g/cm^3.[16]

III. RESULTS

A. Polycrystalline osmium

Polycrystalline materials show only two independent elastic constants (for example, C_{11} and C_{44}), assuming elastic isotropy. Any significant anisotropy would cause our inverse calculation (from frequencies to C_{ij}) to fail. Two independently cut and polished polycrystalline specimens were used to determine C_{11} and C_{44}.

The good agreement between RUS room-temperature results on two specimens leads us to the determination of C_{ij}'s versus temperature for only one polycrystalline specimen. C_{12} was determined from the following relationship (a statement of elastic quasi-isotropy) in the polycrystal:

$$C_{44} = \frac{C_{11} - C_{12}}{2}. \tag{1}$$

1. RUS results for polycrystalline osmium

Results at room temperature and the extrapolated values at 0 K are summarized in Table I. Figure 1 shows the fit of the C_{11}, C_{44} and bulk modulus $[B = C_{11} - (4/3)C_{44}]$ to an Einstein-oscillator model,[17]

$$C_{ij} = C_{ij}^0 - \frac{s}{e^{t/T} - 1}. \tag{2a}$$

Here, *s* is given by the high-temperature near-linear derivative,[18]

TABLE I. Osmium's measured polycrystalline elastic constants at 300 K and extrapolation to 0 K.

Specimen	*T* (K)	C_{11} (GPa)	C_{12} (GPa)	C_{44} (GPa)
*P*1	300	755.7	230.0	262.8
*P*2	300	762.2	229.4	266.4
Average	300	758.9	229.7	264.6
*P*1	0	776.8	234.8	271.1

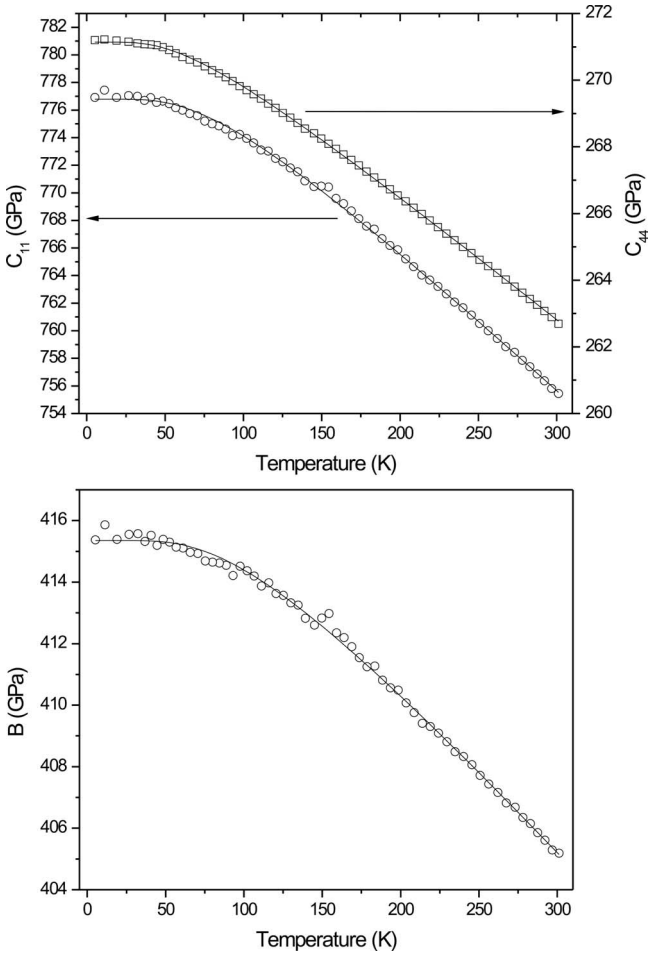

FIG. 1. Polycrystalline-osmium elastic-constant dependence on temperature and their fit to Eq. (2a) derived based on an Einstein oscillator.

TABLE II. C_{ij} fitting parameters to Eq. (2a) for polycrystalline osmium.

Elastic constant	C_{ij}^0 (GPa)	s (GPa)	t (K)
C_{11}	776.8	24.8	233.0
C_{44}	271.1	7.0	182.5
B	415.4	16.6	290.8

$$\frac{\partial C_{ij}}{\partial T} = -\frac{s}{t} = \frac{-3k\gamma(\gamma+1)}{V_a}, \tag{2b}$$

where C_{ij} represents an elastic constant at temperature T, C_{ij}^0 represents an elastic constant at 0 K, t relates to the Einstein temperature, k denotes the Boltzmann constant, γ denotes the Grüneisen parameter, V_a denotes the atomic volume, and s denotes a free parameter. Parameter t is the Einstein temperature. Ledbetter[18] showed later that the parameter s relates to the zero-point-vibration-energy contribution to the elastic stiffness. Equation (2a) was successfully applied to more than 20 materials by Varshni[17] and by us to ZrW_2O_8 (Ref. 19) and diamond.[20] As shown elegantly by Leibfried and Ludwig,[21] the elastic-stiffness temperature dependence can be described using the derivative of any function that describes the internal-energy temperature dependence. [In Ref. 21, see especially their Eqs. (8.16), (13.2), (14.12), (14.13b), and (15.10).] We chose the Einstein function because of its familiarity, analytic simplicity, ease of use, and its excellent agreement with observation. That we used the Debye function to estimate the Debye characteristic temperature from the zero-temperature elastic-stiffness coefficients C_{ijkl} should cause no confusion. We used the Einstein function to extrapolate to the zero-temperature C_{ijkl}. Choosing from any other function would yield the same results especially because $C(T)$ shows an especially small slope near zero temperature because of thermodynamics' third law. Wachtman *et al.*[22] and Varshni[17] considered the $C(T)$ problem for several functions. Ledbetter[6] gave a simple review of $C(T)$ that includes references to contributions by Born, Brillouin, and many others.

The fitting parameters for the polycrystalline elastic constants appear in Table II, while Table III shows the polycrystalline elastic constants and Debye temperatures: bulk-modulus B, shear modulus $G=C_{44}$, Young's modulus E, Poisson ratio υ, and Debye temperature Θ_D. Equations for these appear just below. The Debye temperatures were calculated from the elastic constants and the atomic volume according to Ref. 23,

$$B = \frac{C_{11}+2C_{12}}{3}, \tag{3}$$

TABLE III. Elastic constants and Debye temperatures calculated from the C_{ij}'s of polycrystalline osmium.

T (K)	B (GPa)	G (GPa)	E (GPa)	ν	Θ_D (K)
300	405.2	262.9	648.4	0.233	(467)
0	415.4	271.0	667.8	0.232	474

$$G = C_{44}, \tag{4}$$

$$E = \frac{9BG}{3B+G}, \tag{5}$$

$$\nu = \frac{1}{2}\frac{3B-2G}{3B+2G}. \tag{6}$$

2. *Pulse-echo results for polycrystalline osmium*

From the measured sound speeds v_k, the elastic constants are calculated as follows:

$$C_{ij} = \rho v_k^2. \tag{7}$$

Here C_{ij} denotes the elastic constant for the combination of propagation direction and polarization, ρ denotes the mass density, and v_k denote the sound speeds. The following elastic constants were determined for the polycrystalline specimens: C_{11} (compressional mode or P wave) and C_{44} (shear mode or S wave). Sound speed, elastic constants, and Poisson ratio determined experimentally and/or calculated appear in Table IV. The small differences between the values obtained from RUS and pulse echo can be explained as follows: for a polycrystalline specimen, the pulse-echo method requires two independent measurements of the sound speed in the same propagation direction, using two different polarizations (P wave and S wave), with the two different transducers mounted individually on the specimen, leading to small errors introduced by imperfect parallelism and specimen—bond thickness variation. RUS requires only one measurement: a frequency sweep, which reveals the specimen's macroscopic mechanical resonances. Also, for RUS there is no transducer bond. The first 40 resonances were used to obtain the elastic constants. The pulse-echo method is a good starting point for determining the C_{ij}'s, but RUS should be used for more precise measurements.

B. Monocrystalline osmium

Hexagonal-symmetry monocrystals show five independent elastic constants (C_{11}, C_{12}, C_{13}, C_{33}, and C_{44}). Two in-

TABLE IV. Pulse-echo experimental values for an osmium polycrystalline specimen at 300 K.

v_L (km/s)	v_S (km/s)	C_{11} (GPa)	C_{12} (GPa)	C_{44} (GPa)	B (GPa)	G (GPa)	E (GPa)	ν
5.747	3.425	746.7	216.3	265.2	393.1	265.2	649.6	0.190

TABLE V. Osmium's monocrystalline elastic moduli at a temperature of 300 K and extrapolation to 0 K.

Specimen	T (K)	C_{11} (GPa)	C_{12} (GPa)	C_{13} (GPa)	C_{33} (GPa)	C_{44} (GPa)	C_{66} (GPa)
*S*1	300	747.5	229.0	216.1	816.7	259.2	259.3
*S*2	300	751.6	230.8	219.6	823.1	259.2	260.4
Average	300	749.5	229.9	217.8	819.9	259.2	259.9
*S*1	0	761.7	227.4	217.1	840.1	269.1	267.0
*S*2	0	765.0	228.4	219.0	846.2	269.5	268.3
Average	0	763.3	227.9	218.0	843.2	269.3	267.7

dependently cut and polished monocrystalline specimens were used to determine the above five elastic constants. Because it has more physical meaning (shear on the x_1 plane in the x_2 direction) than C_{12} or C_{13}, we also show the value of C_{66} determined from the hexagonal-symmetry relationship,

$$C_{66} = \frac{C_{11} - C_{12}}{2}. \tag{8}$$

1. RUS results for monocrystalline osmium

The measured C_{ij}'s for the monocrystalline specimens at 300 and 0 K are summarized in Table V. The rms error between measured frequencies and fitted frequencies was 0.1–0.2 % at all temperatures. The difference in elastic constants between the two monocrystals (independently oriented and polished) is less than 1%, with the exception of C_{13}, which shows a slightly higher uncertainty. Note that no sound propagation speed depends solely on C_{13}; C_{13} always occurs in combination with much higher moduli and mostly with negative sign so the error in any sound speed is much less than the error in C_{13} and the temperature dependence is usually opposite to that of diagonal moduli. Henceforth, we focus on the second monocrystalline specimen while noting that all our observations are consistent with the first monocrystalline specimen.

The normalized elastic constants, $C_{ij}(T)/C_{ij}(300\ \mathrm{K})$, dependences on temperature between 300 and 5 K, are shown in Fig. 2. Different elastic constants at selected temperatures are given in Table VI.

Figure 3 shows the fit of selected results to an Einstein-oscillator model.[17] The fitting parameters for selected elastic constants are given in Table VII.

The average-over-direction effective elastic constants were calculated from the monocrystalline elastic constants according to Ref. 23, for a hexagonal-symmetry crystal, and are shown in Table VIII.

2. Pulse-echo results for monocrystalline osmium

Using a pulse-echo method, four of the five independent elastic constants were determined, according to Table IX (see Ref. 24). Because of the good agreement between the results obtained with the two methods (RUS and pulse echo) and the

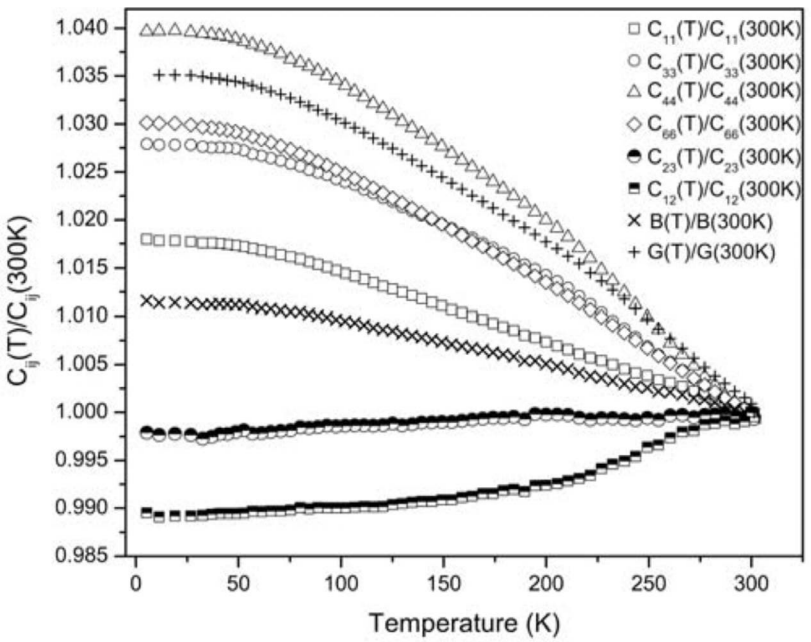

FIG. 2. Osmium's normalized elastic constants versus temperature. Note small changes for all the elastic constants, with larger changes in shear modes than longitudinal modes.

TABLE VI. C_{ij}'s for osmium at selected temperatures.

T (K)	C_{11} (GPa)	C_{12} (GPa)	C_{13} (GPa)	C_{33} (GPa)	C_{44} (GPa)	C_{66} (GPa)	B (GPa)	G (GPa)
301.19	751.54	230.81	219.48	822.85	259.08	260.36	406.81	265.48
282.15	752.67	230.65	219.59	825.20	260.01	261.01	407.32	266.29
260.38	753.90	230.30	219.56	827.75	261.14	261.80	407.76	267.25
243.47	754.67	229.85	219.45	829.83	262.17	262.41	407.99	268.07
221.33	755.84	229.40	219.47	832.64	263.41	263.22	408.44	269.10
199.86	757.10	229.16	219.58	835.10	264.45	263.97	408.96	270.00
178.96	758.26	229.03	219.50	837.00	265.29	264.62	409.36	270.76
158.83	759.34	228.86	219.44	838.68	266.06	265.24	409.71	271.47
139.29	760.45	228.77	219.40	840.26	266.77	265.84	410.08	272.13
120.42	761.42	228.64	219.34	841.75	267.46	266.39	410.40	272.76
101.94	762.43	228.61	219.32	843.10	268.08	266.91	410.76	273.34
79.98	763.53	228.62	219.29	844.46	268.70	267.46	411.14	273.94
61.13	764.21	228.52	219.15	845.36	269.12	267.84	411.30	274.36
40.78	764.74	228.48	219.13	846.09	269.44	268.13	411.48	274.67
19.01	764.98	228.42	219.14	846.30	269.56	268.28	411.54	274.79
5.21	765.09	228.49	219.17	846.38	269.55	268.30	411.61	274.80

observation that RUS values are intrinsically expected to be more accurate, the C_{13} value was not determined using the pulse-echo method. The main obstacle is related to cutting one of the osmium specimens to the correct orientation (45° to the c axis), given the safety and/or health-related issues that can arise with osmium dust. The room-temperature pulse-echo values for the sound speeds and elastic constants are given in Table X.

IV. DISCUSSION

Of the 92 natural elements, 70 are metals at ambient conditions. Among these 70, osmium stands out by showing many remarkable properties: highest hardness, lowest compressibility, highest cohesive energy (after tungsten), highest melting point (after tungsten), and lowest thermal expansivity. As we describe below, osmium shows numerous unusual elastic properties; some are unusual in fitting so closely to ideal simple models. In discussing osmium's elastic properties, we shall use occasionally the concept of *unsaturated* covalent bond (versus the famous saturated covalent bond in diamond where each bond contains two bonding electrons). In terms of the transition metals, Pettifor[25] commented most thoroughly on the bonding issue: "The transition metals are not describable by the conventional nearly free-electron model of the metallic bond since their valence electrons remain relatively tightly bound to their parent atoms, forming unsaturated covalent bonds with their neighbors. These d bonds are responsible for the structural and cohesive properties of the transition metals." Indeed, Pettifor, in his Chap. 7, combined the basic theoretical analysis of bonding in transition metals with bonding in semiconductors. Finally, we should note that osmium is not only unusual mechanically and physically but also chemically; along with ruthenium, osmium is the only element to show all eight oxidation states from +1 through +8, thus enabling a plethora of chemical compounds.

For polycrystalline osmium (Fig. 1), elastic constants change relatively smoothly with temperature, and they are fit well with an Einstein-oscillator model, implying the absence of any significant phase transitions. We associate the small scatter in C_{11} and bulk-modulus B with measurement errors. The change in elastic constants with temperature is small, about 2–3 %, which is expected for a stiff material with high Debye temperature.

Monocrystalline Os shows also smooth behavior with temperature (Fig. 2). The change in the diagonal elastic constants is also small (2–4 %). The off-diagonal terms, C_{12} and C_{13}, show unusual behavior (positive slopes with −0.3% to −1% change), suggesting subtle electronic changes. A closer look (Fig. 3) shows a small deviation around 200 K for some elastic constants. Oscillations in elastic constants were observed previously in cubic-symmetry materials such as Ta, W, Mo, Nb, V, Fe, Pd, Ni, Cu,[26] and Pt.[27] It was argued that the deviations in elastic constants versus temperature arise because these metals go through antiferromagnetic ordering and/or anomalies in thermal expansion.[26] However, the results obtained from thermal expansion, magnetic susceptibility, and specific heat are contradictory, and definite conclusions cannot be drawn. For Pd it was suggested[28] that the nonsmoothness is caused by contributions of the unfilled d band to the elastic constants. Because no abnormal behavior appeared in thermal expansion[13] or in specific heat,[29] most likely the small deviations of C_{ij}'s with temperature arise from small measurement uncertainties introduced by the experimental setup used for cooling or heating.

Agreement between monocrystal-polycrystal measurements and monocrystal measurements obtained by two different methods seems quite good. For the monocrystalline osmium the average percentage differences between RUS

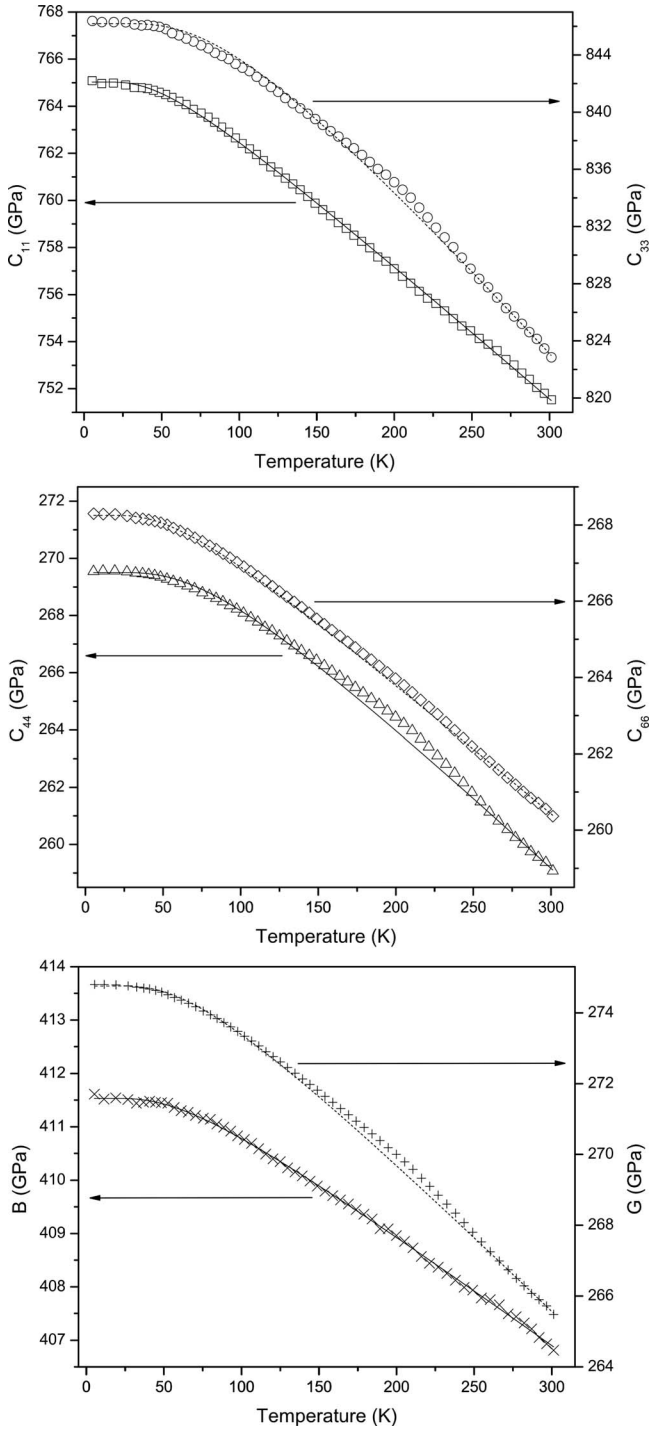

FIG. 3. Selected elastic constants for osmium and their fit to Eq. (2a) based on an Einstein-oscillator model.

and pulse-echo-method values are as follow: (C_{11}) −2%, (C_{12}) −8%, C_{13} is not determined with pulse-echo method, (C_{33}) −1%, (C_{44}) +1%, and (C_{66}) +0.4%. For the polycrystalline osmium the differences are as follow: (C_{11}) −2%, (C_{12}) −6%, and (C_{44}) ±1%. In both cases, all but the off-diagonal terms are within ±2%. As mentioned above, RUS provides more reliable results. More than that the monocrystalline specimen has many advantages over a polycrystal: higher purity, fewer defects, texture absence, and so on.

TABLE VII. Parameters from fitting the measurements to Eq. (2a).

Elastic constant	C_{ij}^0 (GPa)	s (GPa)	t (K)
C_{11}	765.0	8.3	144.1
C_{33}	846.2	32.7	264.8
C_{44}	269.5	11.8	228.8
C_{66}	268.3	5.8	165.3
B	411.5	3.8	180.3
G	274.8	8.6	197.5

We now compare our measurements with *ab initio* theoretical calculations (Table XI). Fast *et al.*[2] used first-principles electronic-structure calculations using the full-potential linear muffin-tin orbital method. Fan *et al.*[3] used the ultrasoft pseudopotential to describe the interaction between ions and electrons. To describe the exchange and correlation potentials, they used the local-density approximation (LDA) and the generalized gradient approximation (GGA). More recently, Minisini *et al.*[4] performed similar calculations but using a projector augmented-wave (PAW) potential for electron-ion interactions. The theoretical values by Fast *et al.* overestimate the C_{ij}'s by 9–21 % [(C_{11}) +17%, (C_{12}) +9%, (C_{13}) +13%, (C_{33}) +21%, and (C_{66}) +21%], except for C_{44}, which is −40% lower than our measurement. Calculations of Minisini *et al.* agree better with our measurements. The percentage differences between averaged LDA and GGA theoretical values and experimental data are (C_{11}) −2%, (C_{12}) +28%, (C_{13}) +1%, (C_{33}) +8%, (C_{44}) +3%, and (C_{66}) −14%. The best agreement between theoretical and experimental values are the calculations by Fan *et al.* with (C_{11}) +0.8%, (C_{12}) −0.5%, (C_{13}) +13.6%, (C_{33}) 0.0%, (C_{44}) −4%, and (C_{66}) +1.4%. However, the value for C_{13} is overestimated by 13.6% and, as pointed by Minisini *et al.*, $C_{13} > C_{12}$ contradicts observation. More advanced theoretical calculations are needed to reconcile the measurement-theory discrepancies and to help understand better osmium's electronic and structural properties. None of the calculations seems to include Pettifor's admonishment that in transition metals unsaturated covalent bonds control interatomic bonding.[25] Some further theory-measurement comparisons occur in our study devoted entirely to the bulk modulus.[30]

Our measurements not only determined osmium's elastic constants at 0 K, which are essential for checking *ab initio* theories, but they also determined the C_{ij}'s temperature dependencies, essential information for checking equations of state and calculations done by methods such as the embedded-atom model.

Although the bulk-modulus (B) for osmium is relatively close to that of diamond (407 and 442 GPa, respectively), its shear modulus (G) is about a half of diamond's (265.6 GPa versus 537.4 GPa).[23] Many (probably most) studies assume that the bulk modulus relates to hardness. Actually, the shear modulus provides a better hardness indicator.[1,7] Hardness depends on dislocation mobility, which in turn depends on the shear modulus G.[7] Osmium's B/G ratio is high (1.5), almost twice than that of diamond (0.8). (A more detailed discussion

TABLE VIII. Average-over-direction (effective polycrystal) elastic constants and derived quantities calculated from the C_{ij}'s: B—bulk modulus, G—shear modulus, E—Young modulus, ν—Poisson ratio, Θ_D—Debye temperature, and A—anisotropy.

Specimen	T (K)	B (GPa)	G (GPa)	E (GPa)	ν	Θ_D (K)	A
*S*1	300	403.4	265.0	652.1	0.231	(469)	1.090
*S*2	300	406.9	265.5	654.3	0.232	(469)	1.093
Average	300	405.1	265.3	653.2	0.231	(469)	1.092
*S*1	0	409.1	273.9	671.7	0.226	476	1.090
*S*2	0	411.5	274.8	674.3	0.227	477	1.090
Average	0	410.3	274.3	673.0	0.227	477	1.090

of osmium's bulk modulus appears in Ref. 30.) Gilman[31] considered the G/B ratio for ten face-centered-cubic metals and found a surprising result that lacks theoretical basis. Gilman observed that as G/B increases these metals move closer to satisfying the Cauchy condition. Indeed, iridium showed the highest G/B, which fell beyond the Cauchy boundary, and thus showed a "negative Cauchy pressure," which is now the focus of many theoretical studies. Gilman concluded that although the crystal structure is simple, the various electron distributions are not so simple, connecting perhaps with Pettifor's unsaturated covalent bond mentioned above. Ledbetter extended Gilman's study to include 23 cubic elements and found eight elements with negative Cauchy pressures.[32] At least for cubic crystals, most simple models predict positive Cauchy pressure. The cubic-symmetry Cauchy condition is $C_{12}=C_{44}$. Showing hexagonal (transverse-isotropic) symmetry, osmium possesses two Cauchy conditions: $C_{13}=C_{44}$ and $C_{11}=3C_{12}$ (equivalently, $C_{12}=C_{66}$). Figure 4 shows the temperature variation in the two Cauchy ratios. Both ratios increase with increasing temperature, tending toward unity at some much higher temperature. The Cauchy discrepancies, usually attributed to many-body forces,[33] are fairly large at the lowest temperatures. For a central-force near-neighbor-only model of hexagonal lattices, Born and Huang[34] derived elastic-constant ratios: $C_{33}:C_{11}:C_{12}:C_{13}:C_{44}:C_{66}=32:29:11:8:8:9$. Beside the central-force and near-neighbor-only departures, Born and Huang took departures from these ratios to reflect internal strains within the hexagonal unit cell. For osmium, these ratios are 32:29:9:8:10:10, reasonably close to the Born-Huang simple model predictions but clearly the small differences are assumed important, as in the Cauchy relationships and in other properties discussed below. In predicting $C_{33}>C_{11}$, the Born-Huang model implies an axial ratio less than the ideal value: 1.633. Osmium shows $c/a=1.5790$. Thus, the closest-packed atoms occur in pairs out of the basal plane rather than in the basal plane, the respective spacings being 2.6754 and 2.7353, and the handbook covalent-bond spacing being slightly lower, 2.56 Å.

TABLE IX. C_{ij} determination procedure using the pulse-echo method.

Propagation mode	Propagation direction	Polarization direction	C_{ij}
Longitudinal	⊥ to c axis		C_{11}
Longitudinal	∥ to c axis		C_{33}
Transverse	∥ to c axis	Any	C_{44}
Transverse	⊥ to c axis	⊥ to c axis	$C_{66}=\frac{1}{2}(C_{11}-C_{12})$

Following the idea of Köster and Franz[35] that the Poisson ratio reveals more about interatomic bonding than any other single elastic constant, we now focus on osmium's anisotropic Poisson ratio. First, we consider osmium's macroscopic (averaged over all directions) Poisson ratio, 0.232, which is lowest among the 30 3*d*-4*d*-5*d* elements, except for Cr (0.212), which possesses magnetic properties that blur the comparison. We argue that low Poisson ratios suggest covalent bonding, as confirmed by the following summary for various element groups in Mendeleev's table:

Noble metals (5)	$\nu=0.383\pm0.030$
Alkali metals (5)	0.359 ± 0.007
Poor metals (10)	0.351 ± 0.087
bcc metals (15)	0.327 ± 0.058
fcc metals (17)	0.325 ± 0.056
Alkaline earths (5)	0.291 ± 0.041
3*d* transition (10)	0.290 ± 0.049
4*d* transition (10)	0.315 ± 0.055
5*d* transition (10)	0.314 ± 0.064
Inert-gas solids (5)	0.297 ± 0.050
Covalent solids (4)	0.167 ± 0.084

The argument becomes more convincing if we examine the Poisson-ratio "tensor," which is defined as follows:

$$\nu_{ij}=-\frac{S_{ij}}{S_{ii}}. \tag{9}$$

Here S_{ij} denote the tensor-inverse components of the C_{ij}, i denotes the stress direction, and j denotes a direction transverse to i. Hexagonal crystals show three principal independent ν_{ij}: ν_{12}, ν_{13}, and ν_{31}. Figure 5 shows the ν_{ij} temperature dependence together with Einstein-oscillator-model best-fit curves. These values are low at zero temperature, that is, 0.196, 0.220, and 0.243, much below the

TABLE X. Pulse-echo measurements for a monocrystalline specimen at 300 K.

C_{11} (GPa)	C_{12} (GPa)	C_{13} (GPa)	C_{33} (GPa)	C_{44} (GPa)	C_{66} (GPa)
734.1	212.4		809.0	262.6	260.8
		Associated sound speed (km/s)			
5.698	N/A[a]		5.982	3.408	3.396

[a]C_{12} lacks an associated sound speed. It was determined from C_{11} and C_{66}.

average for any of the ten material groups shown above. They argue strongly for covalency, especially along the hexagonal axis x_3, the crystal's stiffest direction.

Although the Poison ratio (a ratio of elastic compliances) shows moderate anisotropy, osmium's C_{ij} themselves do not. Indeed, osmium may be the most nearly isotropic element in our experience. The average-over-direction shear-mode anisotropy A at 300 K is 1.093, perfect isotropy being $A=1.000$. (Among the elements, δ Pu shows the highest known elastic anisotropy: 7.03.) Comparing the anisotropy values for $3d$-$4d$-$5d$ hexagonal elements adjacent to osmium, clearly, osmium is most nearly isotropic (Co being 1.49, Re being 1.37, and Ru being 1.17). Osmium shows nearly no shear anisotropy: $C_{44}/C_{66}=0.995$, the relative resistance to shear on the hexagonal basal plane and the prismatic plane, respectively. This near elastic isotropy is surprising because in a nearly free-electron model, as emphasized by Pettifor,[25] some electrons remain near the ion core and retain some of their atomic character. Osmium's atomic electronic structure—$[Xe]4f^{14}5d^{6}6s^{2}$—reveals the key role of d electrons, whose radial-distribution functions consist of highly anisotropic clover-leaf lobes, which one hardly expects to permit near elastic isotropy.

Because the Debye temperature Θ_D connects with so many physical properties, one can estimate it in various ways, the most common being specific heat. However, in an extensive review of various measurement methods, Herbstein[5] concluded that the preferred method is to measure the elastic constants, especially at low temperature. We used our elastic-constant results to calculate osmium's Θ_D by a simple method described elsewhere.[5] We obtained $\Theta_D=477\pm2$ K.[36] Our result settled a long-standing controversy where 20 reported values averaged 411 ± 2 K and ranged from 250 to 500 K. Our result shows consistency with known Θ_D values for adjacent elements in Mendeleev's table. Osmium's Debye temperature exceeds that of all 30 transition metals except Cr and Ru.

We turn now from the quintessential harmonic parameter, the Debye temperature, to the quintessential anharmonic parameter, the Grüneisen parameter γ. Using ambient temperature results for the bulk modulus, the Grüneisen's first rule, and the lattice specific heat, we can calculate the Grüneisen parameter γ as follows:

$$\gamma=\beta\frac{BV_a}{C_p}. \tag{10}$$

Here β denotes the volume thermal expansivity, V_a denotes the unit-cell volume, and C_p denotes the heat capacity. For these properties we took $\beta=15.3\times10^{-6}$ K^{-1}, $V_a=13.9928$ Å^3, and $C_p=24.72$ J K^{-1} mol^{-1}.

Solving Eq. (10) gives $\gamma=2.12$, in good agreement with Gschneidner's value of 2.02.[37] A recent Raman-scattering high-pressure study yielded a mode-Grüneisen parameter of 1.77(12).[38] The extensive review by Gschneidner gives average values of 2.46 ± 0.46 for fcc elements, 1.93 ± 0.42 for close-packed hexagonal (cph) elements, 1.39 ± 0.34 for five

TABLE XI. Osmium's C_{ij}'s. Theory-measurement comparisons.

Source	C_{11} (GPa)	C_{12} (GPa)	C_{13} (GPa)	C_{33} (GPa)	C_{44} (GPa)	C_{66} (GPa)
Fast	894.5	249.2	245.6	1016.4	162.2	322.6
Fan LDA	808.7	243.7	264.7	888.6	271.2	282.5
Fan GGA	730.1	209.8	230.5	798.3	246.9	260.2
Fan avg	769.4	226.8	247.6	843.5	259.1	271.4
Minisini LDA	789	308	239	958	289	240
Minisini GGA	715	274	202	870	265	220
Minisini avg	752	291	220	914	277	230
Expt., present, 0 K	763.3	227.9	218.0	843.2	269.3	267.7

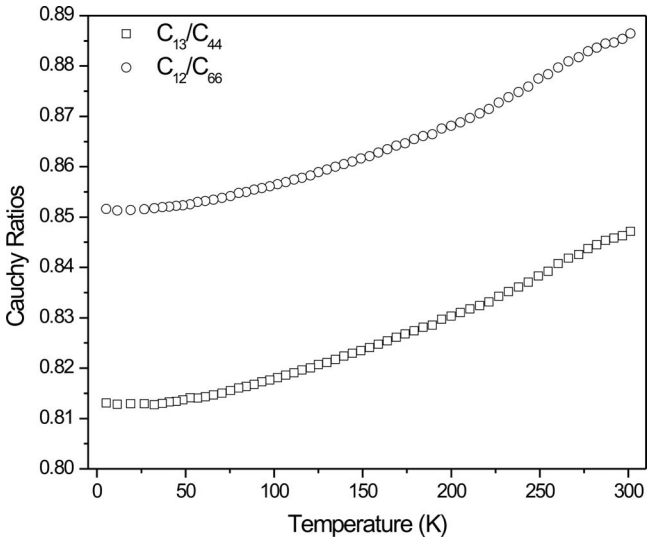

FIG. 4. Temperature variation in two Cauchy ratios C_{12}/C_{66} and C_{12}/C_{44}. If interatomic forces were purely central, these ratios would be equal to 1.000. Their departure from unity is usually ascribed to many-body forces.

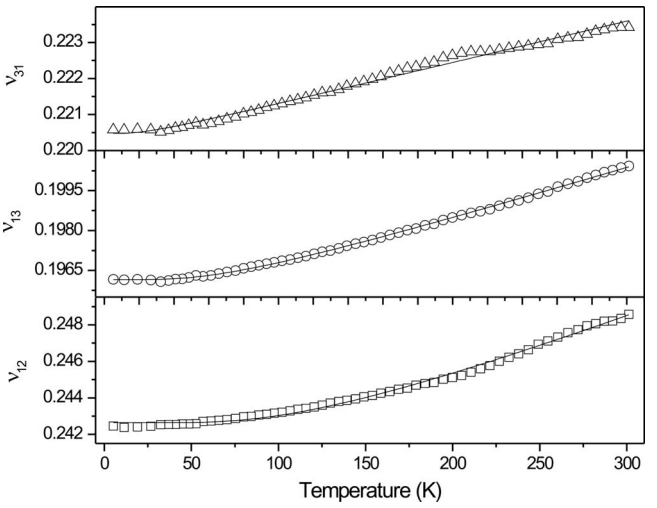

FIG. 5. Temperature variation in the three principal Poison ratios. Slater's argument for positive $d\nu/dT$ slopes is that warming pushes metals toward the liquid state where $\nu=0.5$. The exceptionally low values suggest some covalent bonding. The lowest value, for ν_{13}, suggests that covalent bonds occur out of the basal plane.

alkali metals, and 1.67 ± 0.12 for the remaining bcc metals.[37] Thus, we see that osmium's Grüneisen parameter is about average or very slightly higher.

Solving Eq. (2b) for the Grüneisen parameter gives $\gamma = 2.22$. We can also compare these values with the Grüneisen parameter obtained from the measured dB/dP using the approximate relationship $dB/dP = 2\gamma + 1$. The only data available for dB/dP are from x-ray determination of the bulk modulus from the equation of state: 2.1–5.5, which gives $\gamma = 0.55 - 2.25$.

Finally, we point out that our finding that osmium's bulk modulus exceeds rhenium's indicates some small deficiency in Friedel's popular rectangular-d-band tight-binding model for the transition elements.[39,40] Friedel's model predicts that the bulk modulus shows symmetrical parabolic behavior across a 3d, 4d, or 5d ten-element series. For the 5d series, Friedel predicts rhenium at the apex, whereas we find osmium. Similar difficulties appear in the 3d and 4d series. A possible solution to this problem is to somehow add unsaturated covalent bonds to the theory.

V. CONCLUSIONS

(1) At all studied temperatures, osmium's bulk modulus fails to exceed diamond's, contrary to several previous measurements and *ab initio* theoretical calculations.

(2) Osmium's bulk modulus exceeds that of all other metals (412 GPa at 0 K and 407 GPa at 300 K).

(3) All the elastic constants change smoothly with temperature, fitting well to an Einstein-oscillator model of the $C_{ij}(T)$.

(4) From the low-temperature C_{ij}, we extracted a Debye temperature Θ_D of 477 ± 2 K, highest among the 30 transition metals except for Cr and Ru.

(5) From Grüneisen's first rule, we extracted a Grüneisen parameter γ of 2.12, a moderate value agreeing with handbook values.

(6) Osmium's elastic-stiffness coefficients, the C_{ij}'s, show remarkably low elastic anisotropy, showing anisotropy values near unity for all the usual anisotropy measures.

(7) Osmium's Poisson ratio shows several remarkable features: (i) the lowest average-over-direction value (0.232) among the 30 transition elements; (ii) an especially low out-of-basal-plane value, $\nu_{13}=0.196$; and (iii) considerable anisotropy from 0.196 to 0.243.

(8) Showing a bulk modulus higher than rhenium's goes against Friedel's long-standing tight-binding transition-metal theory.

(9) Several observations support unsaturated covalent bonds in osmium, especially out of the basal plane. These factors include the following: (i) very high bulk modulus, only slightly lower than diamond's, the prototype covalent element; (ii) very low Poisson ratio, both overall and especially in some directions, typical of covalent materials and atypical of metals; (iii) departure from Friedel's tight-binding transition-metal theory, which predicts a too-low value for osmium's bulk modulus; and (iv) small elastic-constant changes with temperature.

[1] D. Clerc and H. Ledbetter, J. Phys. Chem. Solids **59**, 1071 (1998).
[2] L. Fast, J. M. Wills, B. Johansson, and O. Eriksson, Phys. Rev. B **51**, 17431 (1995).
[3] C.-Z. Fan, S.-Y. Zeng, L.-X. Li, Z.-J. Zhan, R.-P. Liu, W.-K. Wang, P. Zhang, and Y.-G. Yao, Phys. Rev. B **74**, 125118 (2006).
[4] B. Minisini, J. Roetting, and F. Tsobnang, Comput. Mater. Sci. **43**, 812 (2008).
[5] H. Herbstein, Adv. Phys. **10**, 313 (1961).
[6] H. Ledbetter, *Materials at Low Temperatures* (American Society for Metals, Metals Park, OH, 1983), p. 1.
[7] J. J. Gilman, Philos. Mag. A **82**, 1811 (2002).
[8] J. J. Gilman, R. W. Cumberland, and R. B. Kaner, Int. J. Refract. Met. Hard Mater. **24**, 1 (2006).
[9] A. Migliori and J. Sarrao, *Resonant Ultrasound Spectroscopy* (Wiley, New York, 1997).
[10] A. Migliori, J. L. Sarrao, W. M. Visscher, T. M. Bell, M. Lei, Z. Fisk, and R. G. Leisure, Physica B **183**, 1 (1993).
[11] J. Maynard, Phys. Today **49**(1), 26 (1996).
[12] O. L. Anderson, J. Acoust. Soc. Am. **91**, 2245 (1992).
[13] Y. S. Toulukian, R. K. Kirby, R. E. Taylor, and P. D. Desai, *Thermal Expansion: Metallic Elements and Alloys*, Thermophysical Properties of Matter Vol. 12 (IFI/Plenum, New York, 1977) p. 244.
[14] C. Pantea, D. G. Rickel, A. Migliori, J. Zhang, Y. Zhao, S. El-Khatib, R. G. Leisure, and B. Li, Rev. Sci. Instrum. **76**, 114902 (2005).
[15] V. A. Finkel', M. I. Palatnik, and G. P. Kovtun, Fiz. Met. Metalloved. **32**, 212 (1971).
[16] *Lange's Handbook of Chemistry*, 14th ed., edited by J. A. Dean (McGraw-Hill, New York, 1992).
[17] Y. P. Varshni, Phys. Rev. B **2**, 3952 (1970).
[18] H. Ledbetter, Phys. Status Solidi B **181**, 81 (1994).
[19] F. R. Drymiotis, H. Ledbetter, J. B. Betts, T. Kimura, J. C. Lashley, A. Migliori, A. P. Ramirez, G. R. Kowach, and J. Van Duijn, Phys. Rev. Lett. **93**, 025502 (2004).
[20] A. Migliori, H. Ledbetter, R. G. Leisure, C. Pantea, and J. B. Betts, J. Appl. Phys. **104**, 053512 (2008).
[21] G. Leibfried and W. Ludwig, *Solid State Physics* (Academic Press, New York and London, 1961), Vol. 12, p. 275.
[22] J. Wachtman, W. Tefft, D. Lam, and C. Apstein, Phys. Rev. **122**, 1754 (1961).
[23] H. Ledbetter, A. Migliori, J. Betts, S. Harrington, and S. El-Khatib, Phys. Rev. B **71**, 172101 (2005).
[24] L. J. Slutsky and C. W. Garland, Phys. Rev. **107**, 972 (1957).
[25] D. Pettifor, *Bonding and Structure of Molecules and Solids* (Oxford University Press, Oxford, 1995), p. 173.
[26] F. H. Featherston and J. R. Neighbours, Phys. Rev. **130**, 1324 (1963).
[27] R. E. Macfarlane, J. A. Rayne, and C. K. Jones, Phys. Lett. **18**, 91 (1965).
[28] J. A. Rayne, Phys. Rev. **118**, 1545 (1960).
[29] V. N. Naumov, I. E. Paukov, G. R. Ramanauskas, and V. Ya. Chekhovskoi, Russ. J. Phys. Chem. **62**, 12 (1988).
[30] C. Pantea, I. Mihut, H. Ledbetter, J. B. Betts, Y. Zhao, L. L. Daemen, H. Cynn, and A. Migliori, Acta Mater. **57**, 544 (2009).
[31] J. Gilman, *Electronic Basis of the Strength of Materials* (Cambridge University Press, Cambridge, 2003), p. 152.
[32] H. Ledbetter, ASA Conference, Salt Lake City, June 2007 (unpublished).
[33] C. Cousins and J. Martin, J. Phys. F: Met. Phys. **8**, 2279 (1978).
[34] M. Born and K. Huang, *Dynamical Theory of Crystal Lattices* (Oxford University Press, London, 1954), p. 149.
[35] W. Köster and H. Franz, Metall. Rev. **6**, 1 (1961).
[36] C. Pantea, I. Stroe, H. Ledbetter, J. B. Betts, Y. Zhao, L. L. Daemen, H. Cynn, and A. Migliori, J. Phys. Chem. Solids **69**, 211 (2008).
[37] K. Gschneidner, *Solid State Physics* (Academic Press, New York and London, 1964), Vol. 16, p. 275
[38] Y. S. Ponosov, I. Loa, V. E. Mogilenskikh, and K. Syassen, Phys. Rev. B **71**, 220301(R) (2005).
[39] J. Friedel, *Physics of Metals* (Cambridge University Press, New York, 1969), p. 494.
[40] D. Pettifor, *Electron Theory in Alloy Design* (Institute of Materials, London, 1992), p. 81.